Supplementary Materials

Lucarelli *et al.,* "Correlating Deep Learning-Based Automated Reference Kidney Histomorphometry with Patient Demographics and Creatinine"

Table of Contents

Augmentation Strategy

The augmentation procedure used to train the panoptic network, and referenced in *Training* of the main manuscript, is defined below in the order that the operations occurred to the image. First, to address variation in staining preparation, we added a random offset to the hue channel (of the HSV space) selected using a random normal distribution centered on zero with standard deviation 0.05. Then, to address brightness variation, we used gamma adjustment on the lightness channel (from the LAB colorspace) selected from a separate random normal distribution centered on one with standard deviation 0.025. Each patch had 90% probability of being subject to this procedure. Next, we used the ImgAug python package to add a number of general augmentation procedures, including elementwise noise, impulse noise, course dropout, Gaussian blurring, and sharpening[1]. The sequence of augmentations was as follows. Sometimes (50% probability), one of elementwise noise (values = (-15, 15), per_channel = 0.5), impulse noise (Pr = 0.05), or course dropout (Pr = 0.02, size_percent = 0.5) was selected randomly and uniformly and applied to the image. Then, sometimes (50% probability), one of Gaussian blur (sigma = (0.0, 3.0)) or sharpening (alpha = (0, 1), lightness = (0.75, 2.0)) was selected uniformly and randomly and applied. Finally, images were subjected to random horizontal flipping with 50% probability, which concluded the augmentation sequence.

Tested Features

Supp. Table 1. **Full list of tested morphometrics and reference values (*N* = 79 subjects, one whole slide image per subject).**

	Institution 1 (*n* = 43)	Institution 2 (*n* = 8)	Institution 3 (*n* = 28)	Combined (*N* = 79)
Patient Characteristics				
Male sex	29 (67.44%)	5 (62.50%)	20 (71.43%)	54 (68.35%)
Age (years)	59.16 ± 11.95	60.63 ± 13.32	53.68 ± 11.94	57.37 ± 12.25
SCr (mg/dL)	1.07 ± 0.24	0.81 ± 0.28 [a]	0.86 ± 0.14 [a]	0.97 ± 0.24
Glomerular histomorphometrics				
Glomeruli (per cortical mm²)	2.59 ± 0.64	1.86 ± 0.57 [a]	2.57 ± 0.80 [b]	2.51 ± 0.72
Average glomerular area (µm²)	18833 ± 3765	23836 ± 6113 [a]	19248 ± 3361 [b]	19487 ± 4134
Standard deviation glomerular area (µm²)	9653 ± 3879	10863 ± 2699	8451 ± 1846	9350 ± 3242
Average glomerular radius (µm)	63.8 ± 6.81	72.08 ± 10.73 [a]	65.93 ± 5.98	65.39 ± 7.33
Standard deviation glomerular radius (µm)	17.08 ± 2.63	19.62 ± 3.74	16.88 ± 2.94	17.27 ± 2.93
Sclerotic glomeruli (per cortical mm²)	0.19 ± 0.14	0.08 ± 0.06	0.24 ± 0.21	0.20 ± 0.17
Average sclerotic glomerular area (µm²)	8252 ± 1712	9222 ± 1883	7780 ± 1579	8188 ± 1713
Standard deviation sclerotic glomerular area (µm²)	4159 ± 1325	5293 ± 3085	2797 ± 1319 [a,b]	3804 ± 1751
Average sclerotic glomerular radius (µm)	42.04 ± 4.66	44.69 ± 5.13	42.62 ± 4.68	42.51 ± 4.72
Standard deviation Sclerotic glomerular radius (µm)	11.56 ± 2.03	13.03 ± 3.45	8.33 ± 3.89 [a,b]	10.59 ± 3.37
Glomerulosclerosis ratio	0.07 ± 0.06	0.04 ± 0.04	0.08 ± 0.07	0.07 ± 0.06
Glomerular proportion of cortex	0.05 ± 0.01	0.04 ± 0.01	0.05 ± 0.01	0.05 ± 0.01
Tubulointerstitial morphometrics				
Tubules (per cortical mm²)	173.53 ± 34.40	132.92 ± 38.17 [a]	189.58 ± 50.16 [b]	175.10 ± 43.57
Average cortical tubular area (µm²)	3269 ± 612	4219 ± 1141 [a]	2476 ± 722 [a,b]	3084 ± 885
Standard deviation cortical tubular area (µm²)	3495 ± 1002	5752 ± 3652 [a]	2809 ± 1232 [b]	3481 ± 1719
Average cortical tubular radius (µm)	20.95 ± 1.53	23.43 ± 2.39 [a]	17.92 ± 2.31 [a,b]	20.13 ± 2.62
Standard deviation cortical tubular radius (µm)	7.65 ± 1.02	8.93 ± 1.67 [a]	7.00 ± 1.38 [b]	7.55 ± 1.33
Average medullary tubular area (µm²)	1768 ± 506	2449 ± 453 [a]	1352 ± 464 [a,b]	1689 ± 579
Standard deviation medullary tubular area (µm²)	2098 ± 1027	3403 ± 1095 [a]	1742 ± 1084 [b]	2104 ± 1141
Average medullary tubular radius (µm)	15.37 ± 1.50	17.75 ± 1.48 [a]	12.69 ± 1.20 [a,b]	14.66 ± 2.13
Standard deviation medullary tubular radius (µm)	5.14 ± 1.01	6.32 ± 0.54 [a]	4.68 ± 0.88 [b]	5.10 ± 1.03
Tubular proportion of cortex	0.55 ± 0.05	0.52 ± 0.07	0.45 ± 0.09 [a,b]	0.51 ± 0.08
Average lumen to wall ratio	0.27 ± 0.05	0.37 ± 0.05 [a]	0.23 ± 0.04 [a,b]	0.27 ± 0.06
Tubular proportion of medulla	0.49 ± 0.10	0.49 ± 0.08	0.38 ± 0.07 [a,b]	0.45 ± 0.10
Interstitial proportion of cortex	0.16 ± 0.10	-0.45 ± 0.13 [a]	0.31 ± 0.06 [a,b]	0.15 ± 0.23
Nephron count	202.79 ± 39.70	149.92 ± 29.42 [a]	218.45 ± 50.52 [b]	202.99 ± 46.74
Interstitial proportion of medulla	0.51 ± 0.10	0.51 ± 0.08	0.62 ± 0.07 [a,b]	0.55 ± 0.10
Vascular morphometrics				
Arteries(ioles) per cortical mm²	5.96 ± 1.59	4.04 ± 1.14 [a]	6.54 ± 1.98 [b]	5.97 ± 1.82
Arter(iole) proportion of cortex	0.04 ± 0.02	0.03 ± 0.01	0.04 ± 0.02	0.04 ± 0.02
Arteriole proportion of medulla	0.03 ± 0.01	0.03 ± 0.02	0.01 ± 0.01 [a,b]	0.02 ± 0.01
Cortical glomerulus to tubule ratio	0.09 ± 0.02	0.08 ± 0.02	0.11 ± 0.02 [a,b]	0.09 ± 0.02

Data are represented as mean ± standard deviation, if not indicated otherwise. *Standard deviation for the population of glomeruli within a single case. [a] Adjusted p-value ≤ 0.05 compared to Institution 1. [b] Adjusted p-value ≤ 0.05 compared to Institution 2.

Performance Analysis

Supp. Table 2A. **Segmentation accuracy comparison to previous study.**

Structure	de Bel *et al.*	Our Study
Viable Glomeruli	0.94	0.999
Globally Sclerotic Glomeruli	0.87	0.999
Tubule	0.94	0.997
Artery/Arteriole	0.78	0.999

Supp. Table 2B. **Segmentation Dice coefficient comparison to previous studies.**

Structure	Bouteldja *et al.*	Hölscher *et al.*	Our Study
Glomeruli	0.934	0.940	**0.999**
Tubule	0.952	0.910	**0.997**
Artery/Arteriole	0.791	0.730	**0.989**

Feature Comparison

Supp. Table 3A. **Feature Measurement Comparison to Previous Study.**

Measurement	Samuel *et al.* (Ages 51-69 years)	Our Study (combined)	Our Study (Institution 1)	Our Study (Institution 2)	Our Study (Institution 3)
Glomerular Volume (μm^3)	$4.86*10^6$ ($1.32*10^6$)	**$3.72*10^6$ ($3.6*10^5$); $p < 0.001$**	**$3.54*10^6$ ($3.2*10^5$); $p < 0.001$**	$5.04*10^6$ ($6.5*10^5$); $p = 0.73$	**$3.65*10^6$ ($2.7*10^5$); $p < 0.001$**
Glomerulosclerosis (%)	4.7 (3.3)	7 (6); $p = 0.20$	7 (6); $p = 0.21$	4 (4); $p = 0.67$	8 (7); $p = 0.13$

Feature measurement comparison to previous study. Feature values are represented as mean (standard deviation). *P* values are compared to Samuel *et al.*, bold values represent significant differences at $p < 0.05$.

Supp. Table 3B. **Feature Measurement Comparison to Previous Study.**

Measurement	Hölscher *et al.*	Our Study (combined)	Our Study (Institution 1)	Our Study (Institution 2)	Our Study (Institution 3)
Glomerular Area (μm^2)	16897 (17307)	19381 (5188)	18817 (5836)	20984 (5926)	18843 (4560)
Tubular Diameter (μm)	30.79 (18.34)	40.73 (6.35)	41.78 (4.05)	47.82 (8.05)	35.58 (6.48)

Feature measurement comparison to previous study. Feature values are represented as median (interquartile range - inclusive).

Supplementary Figures

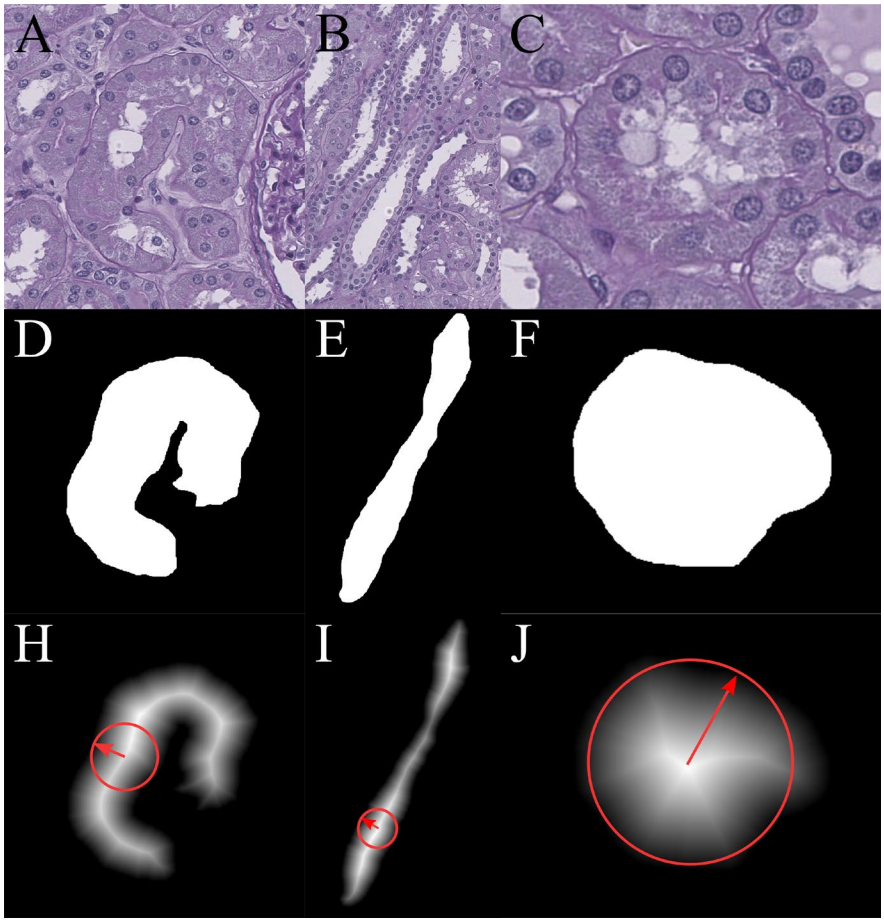

Supp. Fig. 1. **Examples of distance transform applied to various tubular segments.** A-C) Original histology images showing a curled, straight, and cross-sectioned tubule, respectively. D-F) Binary segmentation masks of the tubules in top row. H-J) Distance transformation output, an intensity image with each pixel valued as the distance to closest boundary point. Red arrow and circle annotations correspond to the approximate maximum radius and its circular inscription for each tubule.

Distance transform exemplars

In this work, we chose the distance transform to measure object radius/diameter. ***Supp. Figs. 1A-1C*** show three examples of tubules, one curled unto itself, one straight, and one directly cross-sectioned. The corresponding segmentation masks of these tubules are provided in ***Supp. Figs. 1D-1F.*** The maximum value of the distance transformation identifies the maximum radius of a circle that could be inscribed in the object, as shown in ***Supp. Figs. 1H-1J***. This quantification allows an accurate measurement of the tubular diameter/radius regardless of the angle at which the tubule was sectioned.

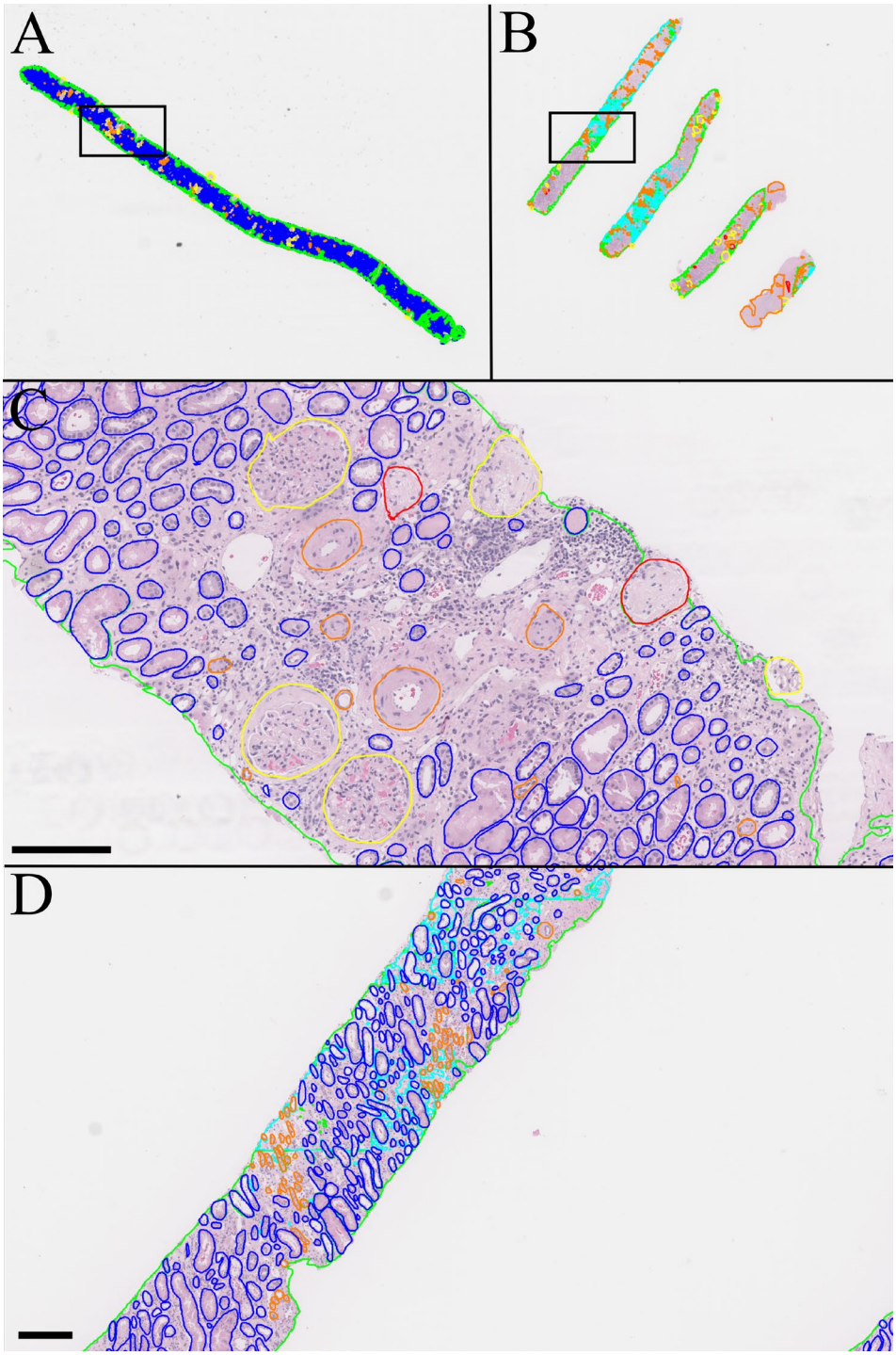

Supp. Fig. 2. **Holdout segmentation of H&E biopsy after inclusion of 23 small training regions totaling 34 mm^2.** A) Thumbnail image of all segmentation boundaries for a biopsy with chronic kidney disease (CKD). B) Thumbnail segmentation of a second biopsy with medulla. C) 12X magnification zoomed inset for the rectangular region in A. D) 4X magnification zoomed inset for the rectangular region in B. Green: cortical interstitium, cyan: medullary interstitium, yellow: viable glomerulus, red: sclerotic glomerulus, blue: tubule, orange: artery/arteriole. Scale bars 150 µm.

Segmentation of other histological stains

We included a limited amount of histological staining other than PAS in the training of our segmentation network. We provide a brief qualitative demonstration of network performance on hematoxylin and eosin (H&E), trichrome, and silver stained kidney with very low training data.

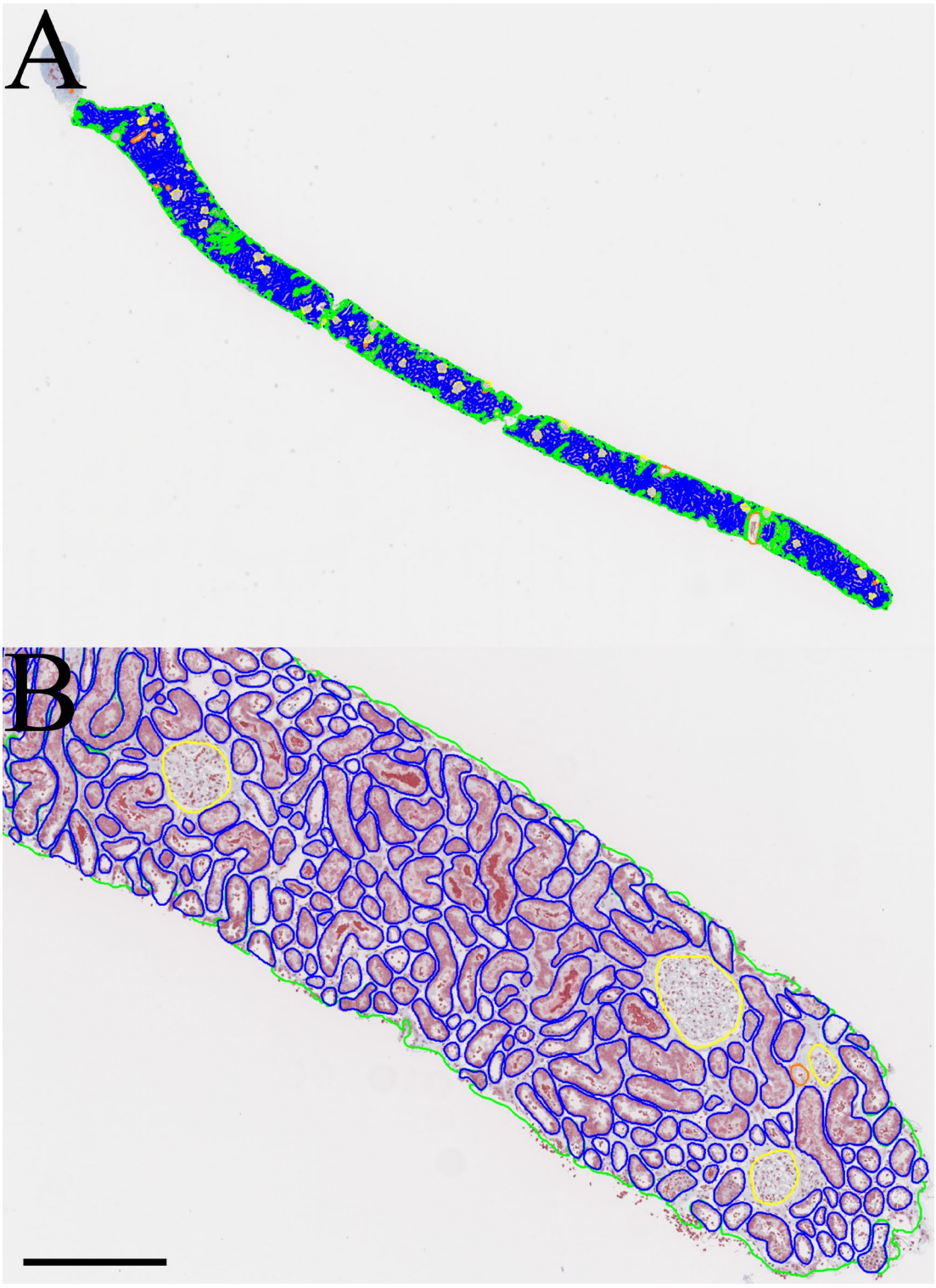

Supp. Fig. 3. **Holdout segmentation of trichrome biopsy after inclusion of four annotated trichrome training patches totaling only 1.4 mm^2 of tissue.** A) Thumbnail image of whole slide predictions. B) Zoomed inset showing individual segmentation boundaries. Green: cortical interstitium, yellow: viable glomerulus, blue: tubule, orange: artery/arteriole. Scale bar 300 µm.

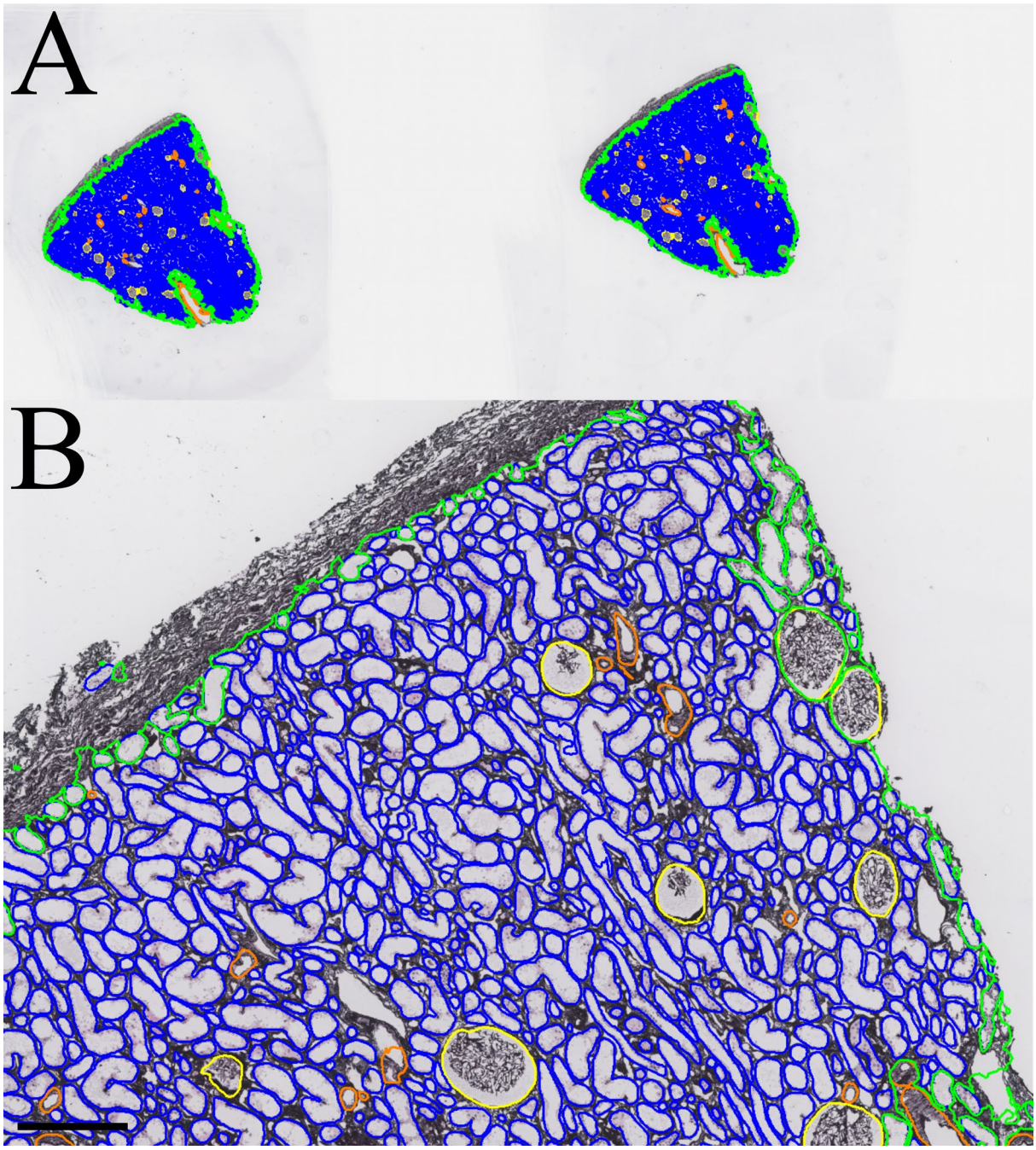

Supp. Fig. 4. **Holdout segmentation of silver biopsy after inclusion of two annotated silver training patches totaling only 2 mm^2 of tissue.** A) Thumbnail image of whole slide predictions. B) Zoomed inset showing individual segmentation boundaries. Green: cortical interstitium, yellow: viable glomerulus, blue: tubule, orange: artery/arteriole. Scale bar 250 μm.

Navigating Whole Slide Images (WSIs) with Annotations in the Digital Slide Archive (DSA)

A User can log in to the Digial Slide Archive (DSA; https://athena.rc.ufl.edu/) as a public user with the following credentials: *Username:* public; *password:* public. The WSIs are located under *Collections/Journals/reference_slides_brightfield_histology_lucarelli_kidney360_2023* (see ***Supp. Fig. 5***). After navigating to the directory, and upon selecting a WSI and clicking on the file name, the user can see the WSI in a separate page with computational annotations in json format and metadata associated with the image under the *Metadata* and *Annotations* section, respectively (see ***Supp. Fig. 6***).

The WSI can be opened by clicking the "*Open in HistomicsUI*" button at the top right (see ***Supp. Fig. 7***). Upon opening the WSI in the HistomicsUI viewer, the user can zoom in and out and hover over regions in the slide to visualize different structures at fine detail.

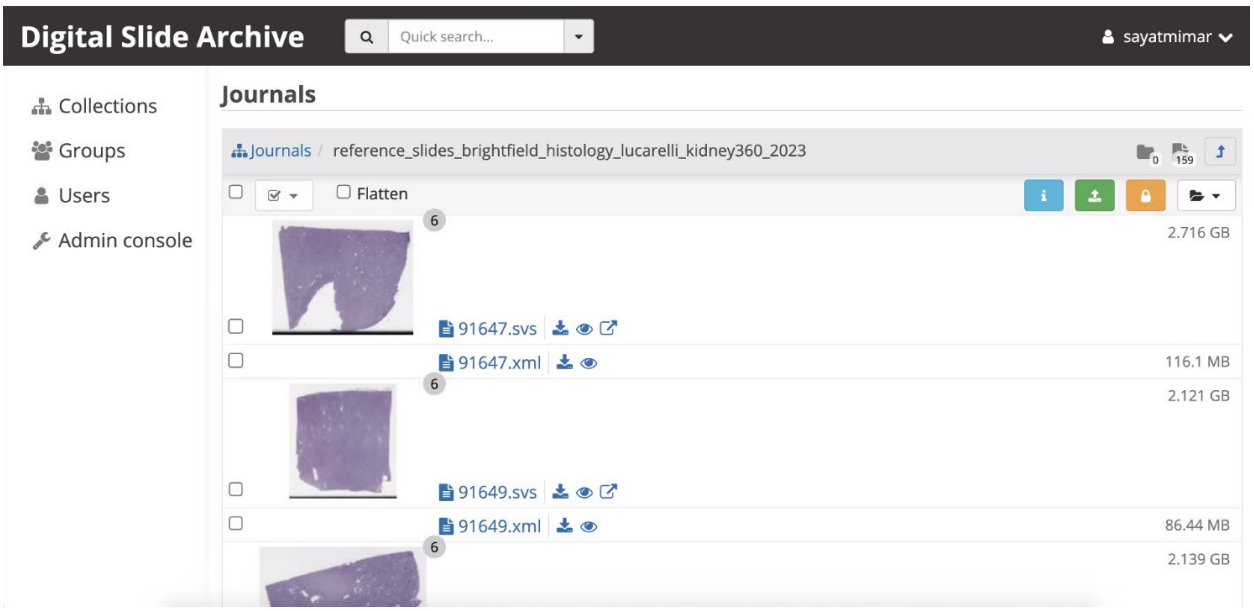

Supp. Fig. 5. **Digital slide archive (DSA).** The WSIs are located under the Collection called *Journals* in the *reference_slides_brightfield_histology_lucarelli_kidney360_2023* directory.

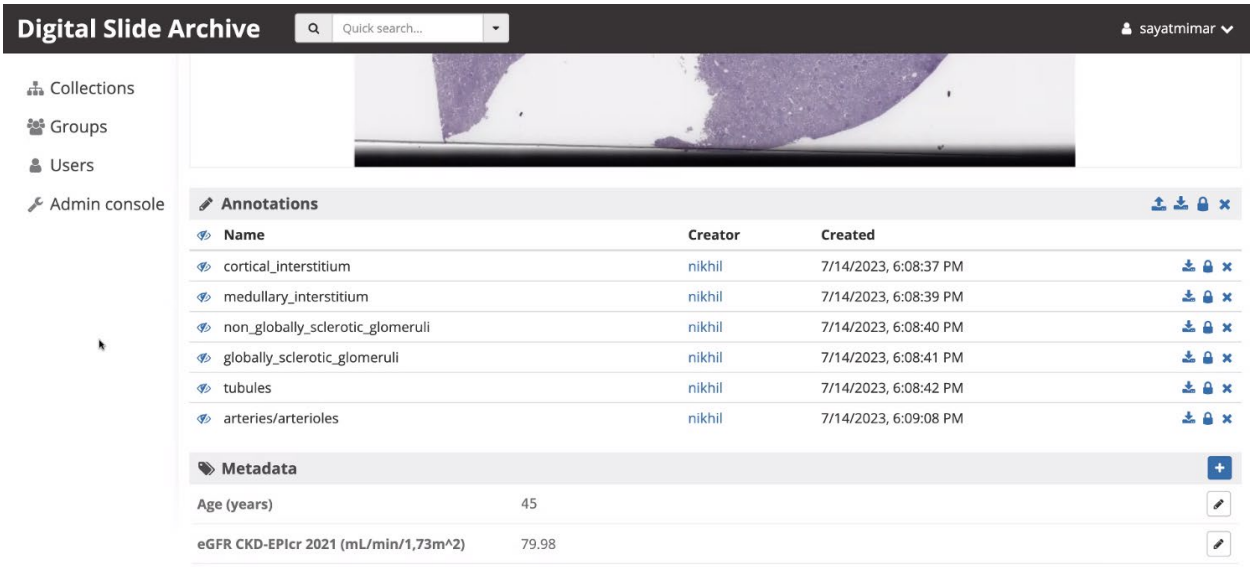

Supp. Fig. 6. **Digital slide archive (Cont.).** Upon opening a WSI in a separate page, downloadable computational segmentation data as well as corresponding non-clinical metadata can be accessed from the same page.

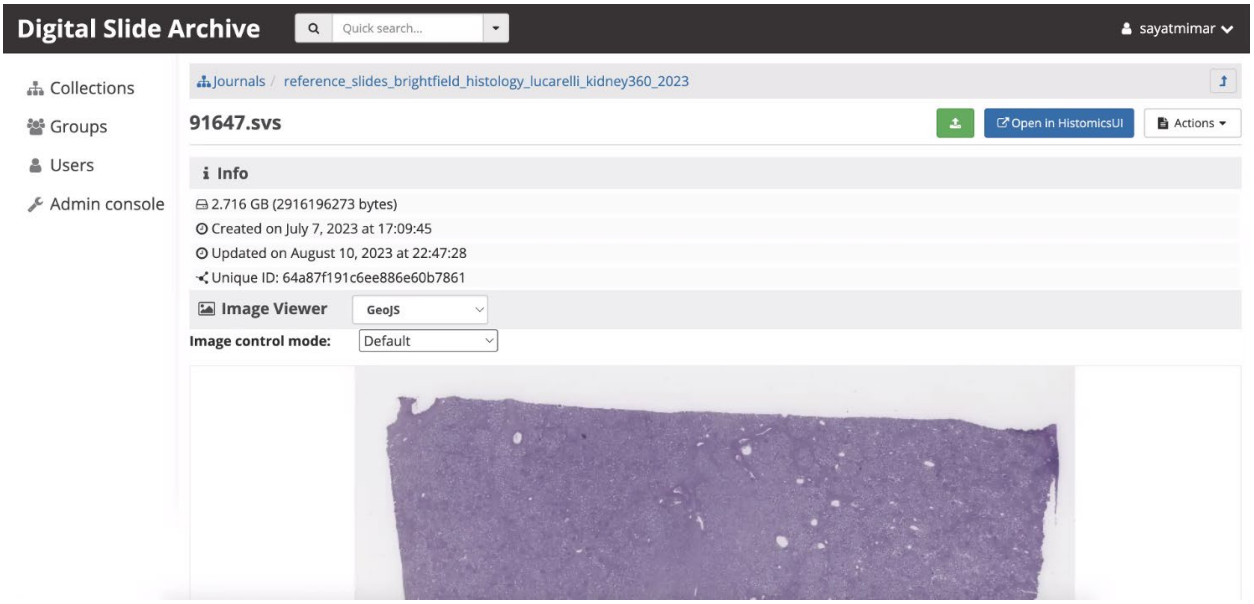

Supp. Fig. 7. **Digital slide archive (Cont.).** Upon clicking and opening a WSI in a separate page, a WSI can be viewed in HistomicUI (a plugin for visualizing large scale image data in cloud via DSA) by clicking '*Open in HistomicsUI*' button.

To visualize the computational annotations, the user must click the *Other* button under the *Annotations* tab which opens six annotations in json format that are of interest in this paper (***Supp. Fig. 8***).

Each compartmental name is written with an eye button; when clicked, users can visualize the corresponding annotation boundaries overlaid on the respective WSI. For example, upon activating the tubules, the boundaries will appear on the WSI (***Supp. Fig. 8B***), and the user can visualize each structure by zooming into the image. It is important to note that due to the large number of annotations being visualized in the cloud for scalable visualization, the rendering of the mask may take a second depending on the server speed. Similarly, users can also visualize other compartments in various colors. For any selected WSI, the multi-compartment segmentation plugin can be run by clicking on *Analyses/sarderlab/ComPRePS/segmentation/MultiCompartmentSegment* (***Supp. Fig. 8A***). Upon selecting the input image file, the base directory where the image is located and the pretrained segmentation model that is located under *models/segmentation_models/Multi_compartment_model,* the job can be submitted. Once the job is run, the segmented annotation will automatically be added under the *Annotations* tab.

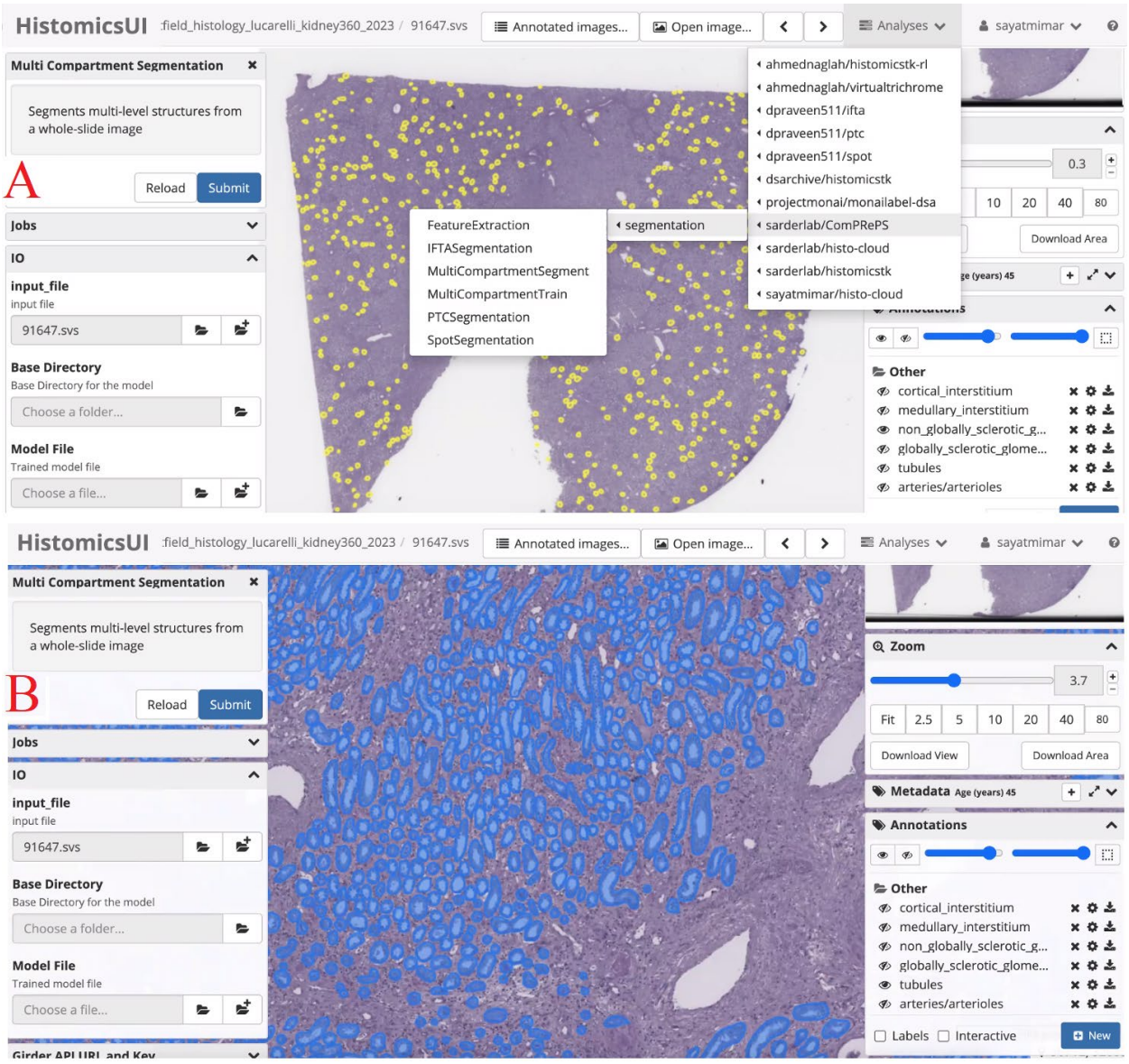

Supp. Fig. 8. **Visualization in HistomicsUI and automated segmentation of renal multicompartments.** Upon opening a WSI in HistomicsUI, computational annotations can be found under the *Other* section within *Annotations*, and can be turned on/off by clicking the eye button on the left. Glomeruli are turned on and represented in yellow as an example in (A). Tubules are represented in blue in (B) and zoomed in for better visualization. The segmentation plugin can be run by clicking on *Analyses/sarderlab/ComPRePS/segmentation/MultiCompartmentSegment,* and populating the tab that opens on the left.